

Tubular Organization with Coiled Ribbon from Amphiphilic Rigid–Flexible Macrocycle

Won-Young Yang, Eunji Lee, and Myongsoo Lee*

Center for Supramolecular Nano-Assembly and Department of Chemistry, Yonsei University, Seoul 120-749, Korea

Received November 17, 2005; E-mail: mslee@yonsei.ac.kr

Self-organization of molecules into helical and tubular architectures provides one of the most significant structural features of proteins and nucleic acids. Inspired by this elegant organization in nature, construction of tubular assemblies has received increasing attention in biomimetic and synthetic supramolecular systems.¹ Artificial tubular structures have been obtained from self-assembly of a wide variety of synthetic scaffolds including peptides,² rigid cycles,³ dendrimers,⁴ and aromatic oligomers⁵ through noncovalent interactions. Self-assembling molecules based on *p*-conjugated rods that mimic lipid amphiphilicity have been proved to be promising scaffolds for electrooptically active 1-D supramolecular structures.⁶ Recently, we have shown that incorporation of a conjugated rod into an amphiphilic dumbbell-shaped molecular architecture gives rise to the formation of a helical nanostructure, consisting of hydrophobic aromatic cores surrounded by hydrophilic flexible segments that are exposed to the aqueous environment.⁷ We have also shown that rod building blocks in rigid–flexible macrocycles self-assemble into a discrete barrel-like structure with hydrophilic channels.⁸

We present here the formation of the tubular objects with coiled ribbons from the self-assembly of conjugated rod building blocks in a rigid–flexible macrocyclic molecule ($f_{\text{coil}} = 0.68$) in aqueous solution (Figure 1). The macrocyclic molecule that forms these aggregates consists of a hexa-*p*-phenylene rod and a chiral poly-(ethylene oxide) chain that are fused together into a macrocyclic ring. The macrocycle was prepared from the cyclization of the allyl-terminated coil–rod–coil precursors by ring-closing metathesis reactions according to procedures reported previously.⁸ The resulting rigid–flexible macrocyclic molecule was characterized by ¹H and ¹³C NMR spectroscopy, elemental analysis, MALDI-TOF mass spectroscopy, and gel permeation chromatography (GPC) and was shown to be in full agreement with the structures presented.

As shown in Figure 2, the molecule in bulk state was observed to self-organize into a 2-D body-centered rectangular structure ($a = 4.3$ nm and $b = 6.3$ nm) that melts into a liquid crystal phase at 127 °C. The transmission electron microscopy (TEM) images showed organized dark, more stained 1-D aromatic domains with a thickness of 2.5 nm. Considering the cyclic molecular structure and aromatic rod length (2.4 nm by CPK), the dark aromatic domains in the image suggest a laterally coupled bilayer ribbon structure in which the rod segments face each other.

The macrocyclic molecule, when dissolved in a selective solvent for one of the blocks, can self-assemble into an aggregate structure because of its amphiphilic characteristics.⁶ Aggregation behavior of the molecule was subsequently studied in aqueous solution by using circular dichroism (CD) spectra. CD spectra of the aqueous solutions of the molecule above certain concentrations (from 0.005 wt %) show first a negative Cotton effect followed by a positive Cotton effect at higher wavelength with the CD signal passing through zero near the absorption maximum of the chromophore (Figure 2d), indicating the formation of a helical superstructure with a preferred handedness.⁹

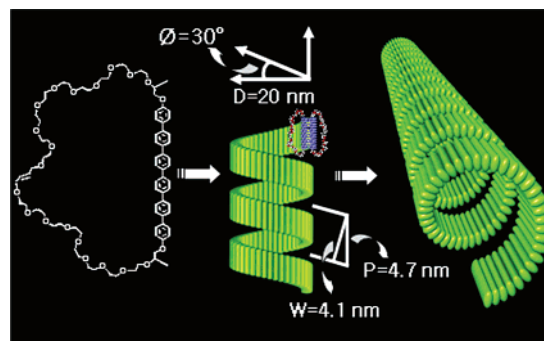


Figure 1. Schematic representation of a proposed mechanism for the formation of the helical tubular structure of **1**.

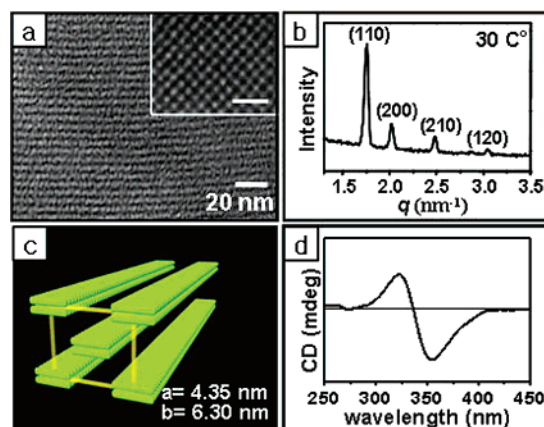


Figure 2. (a) TEM images of ultramicrotomed films **1** stained with RuO₄ revealing columnar array of alternating light-colored PEO layers and dark aromatic layers. (Inset) Image at perpendicular beam incidence; a 2-D body-centered rectangular ordered array of aromatic core (Scale bar: 10 nm). (b) Small-angle X-ray diffraction pattern of **1** measured at 30 °C. (c) Schematic representation for the formation of the 2-D body-centered rectangular columnar structure of **1**. (d) CD spectrum of **1** in aqueous solution (0.005 wt %) at 25 °C.

Dynamic light scattering (DLS) experiments were performed in aqueous solution to further investigate the aggregation behavior.¹⁰ The CONTIN analysis of the autocorrelation function shows a broad peak corresponding to an average hydrodynamic radius of approximately 196 nm. The angular dependence of the apparent diffusion coefficient (D_{app}) was measured because the slope is related to the shape of the diffusing species. The slope was observed to be 0.026, consistent with the value predicted for cylindrical aggregates (0.03).¹¹ The formation of cylindrical aggregates was further confirmed by the Kratky plot that shows a linear angular dependence over the scattering light intensity of the aggregates.¹²

The evidence for the formation of the 1-D cylindrical aggregates was also provided by transmission electron microscopy (TEM) experiments (Figure 3). The micrographs with unstained samples show cylindrical aggregates with lengths up to several micrometers

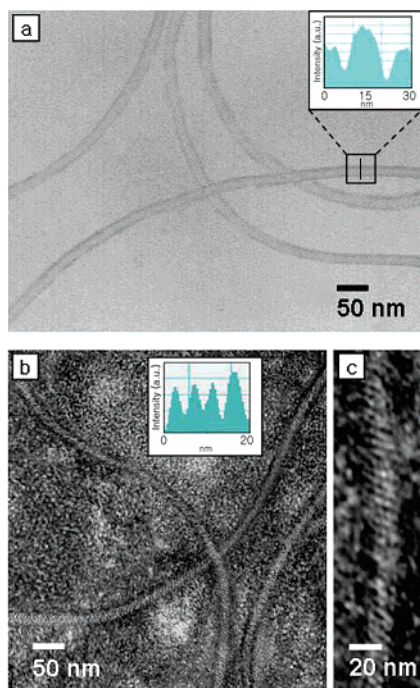


Figure 3. TEM images of (a) the unstained tubular structure of **1** with density profile inset. (b) Negatively stained left-helical tubular structure of **1** with density profile inset. (c) Magnification of the left-helical tubular structure.

and a uniform diameter of about 20 nm (Figure 3a). Notably, there is obvious contrast between the periphery and center in the cylindrical object, characteristic of the projection images of tubular aggregates. The internal diameter and the wall thickness are 14 and 3 nm, respectively, as confirmed by the density profiles taken normal to the long axis of individual objects. When the samples are negatively stained with a 2 wt % aqueous solution of uranyl acetate, the images show the tubular structure with a left-handed helical arrangement with a regular pitch (Figure 3b). The density profiles taken parallel to the long axis of a helical aggregate confirmed the pitch length to be 4.7 nm. The magnified images with negatively stained samples show the elementary ribbons with a uniform width of about 4 nm that is smaller than the extended molecular length (4.8 nm by CPK).¹³ Therefore, it can be considered that the rods are tilted with respect to the ribbon normal with an angle of 33° that is consistent with a pitch angle (30°) obtained from TEM (Figure 3c). Considering this width of single strand (4 nm) along with the pitch angle of 30°, the helical pitch of 4.7 nm suggests that the tubular object is formed by the rolling up of an elementary ribbonlike object.¹³

On the basis of these results, the rod segments can be considered to self-assemble into 1-D ribbonlike aggregates with a laterally stacked bilayer encapsulated by cyclic aliphatic chains in which the rod building blocks are tilted with respect to the ribbon normal at the initial stage. This is supported by molecular dimensions, lattice constants determined from SAXS, and the width of the elementary strand in TEM. However, space crowding of coil segments would be larger in flat ribbonlike aggregates. A ribbonlike ordering of the rod segments would confine flexible coil segments

to a flat interface, which forces a strong deformation of the flexible coils. To release this deformation without sacrificing a parallel arrangement of the rod segments, the flat ribbons would roll up to form a helical tubular structure.¹⁴ This estimation is further supported by the fact that a helical pitch (4.7 nm) of the tubular structure is in reasonable agreement with the extended molecular length. It should be noted that the wall thickness of the tubule (3 nm) is consistent with $b/2$ (3.15 nm) obtained from SAXS.

In summary, the results described here demonstrate that the rigid-flexible macrocycle based on a hexa-*p*-phenylene self-assembles into well-defined ribbonlike aggregates with a rod tilt relative to the ribbon normal at the initial stage. These elementary strands are further coiled with a preferred handedness to form a helical tubular structure with a uniform diameter of about 20 nm and a regular pitch of 4.7 nm. The primary driving force responsible for the formation of the tubular structure with a coiled ribbon is believed to be the energy balance between repulsive interactions among the adjacent flexible chains and π - π stacking interactions. Such a well-defined coiled ribbon arrangement of conjugated rod building blocks may provide a new strategy for the design of hollow 1-D nanomaterials with biological and electrooptical functions.

Acknowledgment. We gratefully acknowledge the National Creative Research Initiative Program of the Korean Ministry of Science and Technology for financial support of this work. E.L. thanks the Seoul Science Fellowship program.

Supporting Information Available: Detailed synthetic procedures, characterization, XRD, TEM, and DLS data. This material is available free of charge via the Internet at <http://pubs.acs.org>.

References

- (1) (a) Shimizu, T.; Masuda, M.; Minamikawa, H. *Chem. Rev.* **2005**, *105*, 1401–1444. (b) Bong, D. T.; Clark, T. D.; Granja, J. R.; Ghadiri, M. R. *Angew. Chem., Int. Ed.* **2001**, *40*, 988–1011. (c) Hill, D. J.; Mio, M. J.; Prince, R. B.; Hughes, T. S.; Moore, J. S. *Chem. Rev.* **2001**, *101*, 3893–4012. (d) Hill, J. P.; Jin, W.; Kosaka, A.; Fukushima, T.; Ichihara, H.; Shimomura, T.; Ito, K.; Hashizume, T.; Ishii, N.; Aida, T. *Science* **2004**, *304*, 1481–1483.
- (2) Gellman, S. H. *Acc. Chem. Res.* **1998**, *31*, 173–180.
- (3) (a) Ryu, J.-H.; Oh, N.-K.; Lee, M. *Chem. Commun.* **2005**, 1770–1772. (b) Höger, S. *Chem. Eur. J.* **2004**, *10*, 1320–1329. (c) Zhao, D.; Moore, J. S. *Chem. Commun.* **2003**, 807–818.
- (4) Percec, V.; Dulcey, A. E.; Balagurusamy, V. S. K.; Miura, Y.; Smidrkal, J.; Peterca, M.; Nummelin, S.; Eödlund, U.; Hudson, S. D.; Heiney, P. A.; Duan, H.; Magonov, S. N.; Vinogradov, S. A. *Nature* **2004**, *430*, 764–768.
- (5) (a) Nelson, J. C.; Saven, J. G.; Moore, J. S.; Wolynes, P. G. *Science* **1997**, *277*, 1793–1796. (b) Petitjean, A.; Nierengarten, H.; van Dorsselaer, A.; Lehn, J.-M. *Angew. Chem., Int. Ed.* **2004**, *43*, 3695–3699. (c) Kim, H.-J.; Zin, W.-C.; Lee, M. *J. Am. Chem. Soc.* **2004**, *126*, 7009–7014. (d) Ryu, J.-H.; Bae, J.; Lee, M. *Macromolecules* **2005**, *38*, 2050–2052.
- (6) Lee, M.; Cho, B.-K.; Zin, W.-C. *Chem. Rev.* **2001**, *101*, 3869–3892.
- (7) Bae, J.; Choi, J.-H.; Yoo, Y.-S.; Oh, N.-K.; Kim, B.-S.; Lee, M. *J. Am. Chem. Soc.* **2005**, *127*, 9668–9669.
- (8) Yang, W.-Y.; Ahn, J.-H.; Yoo, Y.-S.; Oh, N.-K.; Lee, M. *Nat. Mater.* **2005**, *4*, 399–402.
- (9) Ky Hirschberg, J. H. K.; Brunsveld, L.; Ramzi, A.; Vekemans, J. A. J. M.; Sijbesma, R. P.; Meijer, E. W. *Nature* **2000**, *407*, 167–170.
- (10) See Supporting Information.
- (11) Gohy, J.-F.; Lohmeijer, B. G. G.; Alexeev, A.; Wang, X.-S.; Manners, I.; Winnik, M. A.; Schubert, U. S. *Chem. Eur. J.* **2004**, *10*, 4315–4323.
- (12) Bockstaller, M.; Köhler, W.; Wegner, G.; Vlassopoulos, D.; Fytas, G. *Macromolecules* **2000**, *33*, 3951–3953.
- (13) See Supporting Information.
- (14) The observed supramolecular handedness is believed to arise from steric constraints imposed by the chiral centers in the poly(ethylene oxide) chain.

JA057823E